



	Experiment title: Misfit dislocation gettering by substrate pit-patterning in SiGe films on Si(001)	Experiment number: MA-1703
Beamline: ID01	Date of experiment: from: 17/04/2013 to: 24/04/2013	Date of report: 31/08/2013
Shifts: 18	Local contact(s): Tobias Schüllli, Peter Boesecke	<i>Received at ESRF:</i>

Names and affiliations of applicants (* indicates experimentalists):

Daniel Chrastina^{1*}, Valeria Mondiali^{1*}, Stefano Cecchi^{1*}, Monica Bollani^{2*}, Jacopo Frigerio¹, Giovanni Isella¹, Francesca Boioli³, Francesco Montalenti³

1. L-NESS Politecnico di Milano, Dip. di Fisica, Via Anzani 42, I-22100 Como, Italy
2. CNR-IFN, L-NESS, via Anzani 42, I-22100 Como, Italy
3. Dipartimento di Scienza dei Materiali, Università degli Studi di Milano-Bicocca, Via Cozzi 53, I-20125 Milano, Italy

Report:

Using high-resolution x-ray nanodiffraction, we aimed to map the local uniaxial strain fields induced by misfit dislocations in SiGe/Si heterostructures. It has been shown that epitaxial deposition of a low-misfit $\text{Si}_{1-x}\text{Ge}_x$ film on top of a Si(001) substrate patterned with {111}-faceted pits oriented in a square network along the $\langle 110 \rangle$ directions leads to trapping of misfit dislocations. Thin Si-rich SiGe films were therefore deposited on periodic and aperiodic templates realized on Si(001) substrates (Fig. 1a), and laboratory atomic-force microscopy (AFM) was used to check that crosshatch lines were associated with pits (Fig. 1b).

At ID01, a 8.47 keV beam was used. This energy was chosen so that the exit angle for the asymmetric (113) reflection would be extremely grazing (1.3° for Si), such that the diffracted signal would come from a region very close to the surface where the relevant effects are expected to be seen. The incidence angle for (113) was around 52° , which maintained a small beam footprint on the sample, and was close to the limit of collision between the optical microscope objective and the x-ray focusing optics. The symmetric (004) reflection was also accessible. A Fresnel zone plate was used and a spot diameter of about 500 nm was obtained.

Using a newly-developed fast scan mode, diffraction intensity maps in real space were obtained and compared with surface topography maps obtained by AFM. The fast scan mode allows 2-dimensional intensity maps to be obtained extremely quickly as compared to the previously-used method of step-wise scanning, detector image acquisition, and reconstruction (see, for example, experiments SI-1873 and HS-4672) and therefore allows structures within the sample to be immediately identified in detail. The use of an aperiodic pattern allowed direct correlation between AFM (Fig. 2a) and diffracted intensity maps (Fig. 2b). A $20 \times 20 \mu\text{m}^2$ area of the pattern is shown in Fig. 3, which demonstrates direct correlation between surface topography and diffracted intensity. Images of the diffracted beam were recorded over a range of incidence angles close to both Si and SiGe (004) and (113) Bragg conditions (Fig. 4), so that strain and tilt could be reconstructed in both the substrate and SiGe film using symmetric and asymmetric three-dimensional reciprocal space mapping. These results will eventually be compared with Finite Element Method (FEM) models and micro-Raman spectroscopy results.

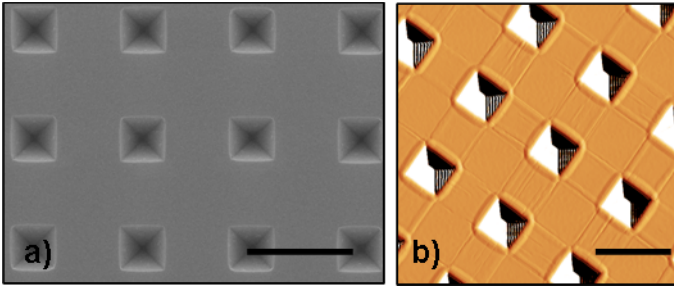


Fig. 1. (a) SEM image of a periodic pattern made up of an array of inverted $\{111\}$ -faceted pyramids before the deposition of a SiGe layer. The pitch is $2.5 \mu\text{m}$, the distance between the inverted pyramids is about $1.5 \mu\text{m}$ and the pyramid width is about $1 \mu\text{m}$. (b) AFM tapping amplitude image of a periodic pattern made up of an array of inverted $\{111\}$ -faceted pyramids after deposition of a 250 nm thick $\text{Si}_{0.8}\text{Ge}_{0.2}$ layer. The image area is about $10 \times 10 \mu\text{m}^2$. The lines

connecting the pits are attributed to bunches of misfit dislocations at the Si/SiGe interface. According to the surface topography, misfit dislocations run along pit rows while the regions between rows remain dislocation free.

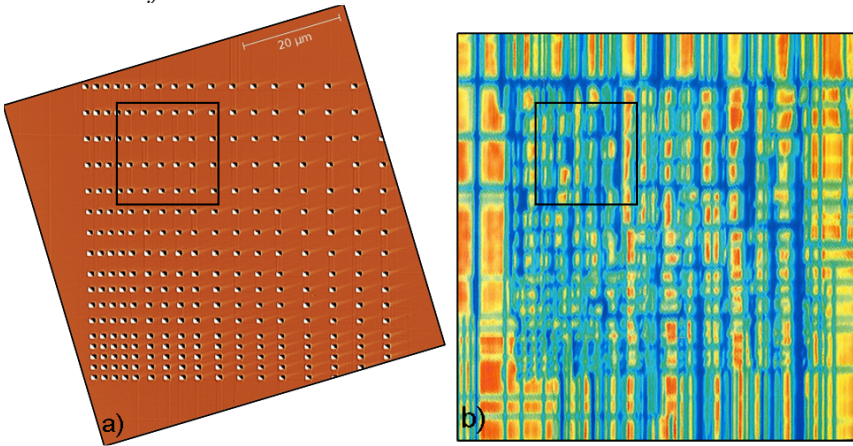


Fig. 2. (a) AFM tapping amplitude image of an aperiodic pattern made up of an array of inverted $\{111\}$ -faceted pyramids after deposition of a 250 nm thick $\text{Si}_{0.85}\text{Ge}_{0.15}$ layer. The pitch increases from 2 to $5 \mu\text{m}$. The patterned area is about $60 \times 60 \mu\text{m}^2$. A $20 \times 20 \mu\text{m}^2$ square marks the area shown in Fig. 3a. (b) X-ray diffraction intensity real space map taken at the (113) Bragg condition of the SiGe film over the same area. The same features can be identified in both images, both

within and outside the aperiodic pattern itself. In particular, apart from the pits themselves, crosshatch lines in the AFM image correspond to regions of lower intensity in the X-ray map. The X-ray beam is incident from the right of the image.

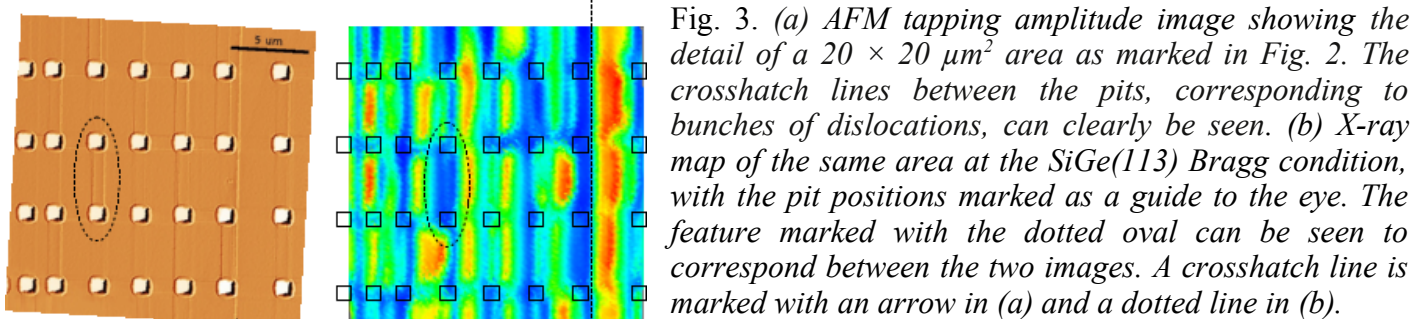


Fig. 3. (a) AFM tapping amplitude image showing the detail of a $20 \times 20 \mu\text{m}^2$ area as marked in Fig. 2. The crosshatch lines between the pits, corresponding to bunches of dislocations, can clearly be seen. (b) X-ray map of the same area at the SiGe(113) Bragg condition, with the pit positions marked as a guide to the eye. The feature marked with the dotted oval can be seen to correspond between the two images. A crosshatch line is marked with an arrow in (a) and a dotted line in (b).

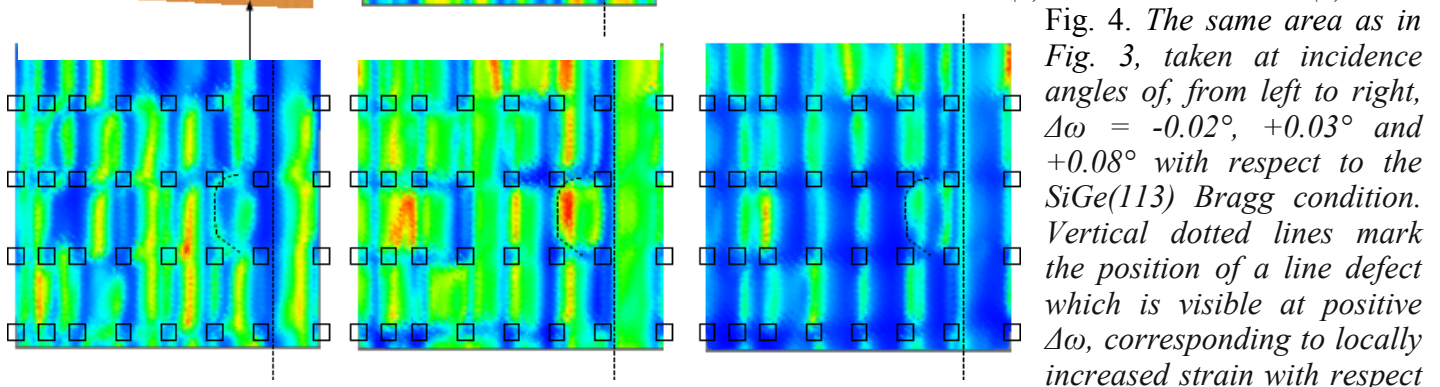


Fig. 4. The same area as in Fig. 3, taken at incidence angles of, from left to right, $\Delta\omega = -0.02^\circ$, $+0.03^\circ$ and $+0.08^\circ$ with respect to the SiGe(113) Bragg condition. Vertical dotted lines mark the position of a line defect which is visible at positive $\Delta\omega$, corresponding to locally increased strain with respect

to the SiGe layer. This line is marked with an arrow in Fig. 3(a).

Figs. 3 and 4 show locally increased strain in the SiGe layer below a crosshatch line. Comparison with results obtained in the (004) geometry will allow the effects of tilt and strain to be separated, and consideration of misfits running within or perpendicular to the beam scattering plane will allow the evaluation of strain in both in-plane directions. Strong support from the beamline staff is gratefully acknowledged, especially in terms of the development of the fast-scan mode and the processing of the resulting intensity maps.